Journal of Marine Science and Application (2022) 21: 116-127
https://doi.org/10.1007/s11804-022-00257-y

RESEARCH ARTICLE

Optimization of a Dual-Baffled Rectangular Tank Against the Sloshing Phenomenon

Hassan Saghi[1,2], Dezhi Ning[2], Shunqi Pan[2,3] and Reza Saghi[4]

Received: 03 September 2021 / Accepted: 24 October 2021

Abstract

A dual-baffled rectangular tank with different configurations is proposed to reduce the sloshing effect, and design optimization is conducted through numerical simulations with open-source software, namely OpenFOAM, based on the computational fluid dynamic model. A series of physical experiments in the dual-baffled rectangular tank is performed for model validation and design optimization with the measured water surface elevation distributions along the tank. The optimization uses the calculated maximum horizontal force exerted on the tank and entropy generation (EG) as the criterion. Results show that the dual-baffle configuration positioned at the tank center is more effective in reducing the sloshing than that of the single baffle when the relative baffle height and initial water depth ratio (H_b/H_w, where H_b and H_w represent baffle height and static water depth, respectively) are larger than 0.5. However, such an effect then diminishes when the ratio is larger than 0.75. The effect of the dual-baffle configuration on the sway motion under the condition of different motion amplitudes and frequencies is also evaluated. The results show that the reduction in the maximum horizontal force is almost the same for dual- and single-baffled configurations and reaches the minimum when the sway motion amplitude is near 0.03 m. The dual-baffled configuration for the angular frequency of the sway motion is more effective than the single-baffled in reducing the sloshing at the low angular frequencies but is only less effective at high angular frequencies. Furthermore, the optimal baffle inclination angle is 85° when the inclined straight and curved baffles are used, and curved baffles can successfully decrease the horizontal force exerted on the tank and EG.

Keywords Rectangular storage tank; Dual-baffled rectangular tank; Sloshing phenomenon; Optimization;Horizontal force; Entropy generation

Article Highlights

- A numerical model was developed to model the sloshing in tank.
- The effectiveness of dual- and single-baffled configurations were compared in reducing the sloshing impact.
- The inclined and curved dual-baffle configurations were optimized.
- Find the optimum aspect ratio of the tank based on entropy generation as a new criterion to compare different scenarios.

✉ Dezhi Ning
dzning@dlut.edu.cn

[1] Department of Civil Engineering, Hakim Sabzevari University, Sabzevar 9617976487, Iran

[2] State Key Laboratory of Coastal and Offshore Engineering, Dalian University of Technology, Dalian 116024, China

[3] Hydro-environmental Research Centre, School of Engineering, Cardiff University, Cardiff CF24 3AA, UK

[4] MSc of Hydraulic engineering, Mashhad Branch, Islamic Azad University, Mashhad 9187147578, Iran

1 Introduction

Fluid sloshing is a free surface oscillation of the contained fluid due to the impulsive loads in a partially filled tank (Abramson 1996). This phenomenon is one of the major concerns in the design of dynamic systems, such as aerospace vehicles, road tankers, seagoing vessels, liquefied natural gas carriers, elevated water towers, and cylindrical petroleum tanks. Numerical and experimental studies on sloshing have been performed by many researchers. The fluid was considered to be inviscid (Frandsen 2004; Ketabdari and Saghi 2012a; 2012b; Ketabdari and Saghi 2013a; 2013b; 2013c; Ketabdari and Saghi 2015; Saghi 2016; Saghi and Ketabdari 2012) and viscous (Chen and Nokes 2005; Wu et al. 2012) in the numerical modeling. Therefore, Laplace and Reynolds-averaged Navier–Stokes (RANS) equations were used as governing equations. The shape of the storage tank is another important concern in

the modeling of sloshing. The performance of different geometric shapes of storage tanks, such as trapezoidal (Ketabdari and Saghi 2015), circular conical (Gavrilyuk et al. 2005), elliptical (Hashemian and Aghabeigi 2012), rectangular (Saghi and Lakzian 2017; Saghi et al. 2020a; Saghi et al. 2021), cylindrical (Papaspyrou et al. 2004; Shekari et al. 2009), and spherical (Yue 2008; Curadelli et al. 2010), were investigated. For example, Saghi and Lakzian (2017) numerically studied the sloshing phenomenon in rectangular tanks with different dimensions to find the optimum aspect ratio of the tank based on some criteria, including entropy generation. The baffles have been widely used in the storage tanks to alleviate the sloshing-induced forces on storage tanks and damp out the sloshing. Some researchers used the baffles with different locations and shapes as a promising way to reduce the sloshing impact. Therefore, Ning et al. (2012) exerted the coupled vertical and horizontal motions on a vertical baffled rectangular storage tank. The sloshing phenomenon in the work of Jung et al. (2012) was modeled in a rectangular tank with different baffle heights and water depths. They found that the free surface oscillation was minimized when the ratio of baffle height to water depth was around 0.9. Nayak and Biswal Kishore (2015) numerically simulated the seismic response of rectangular liquid tanks with a bottom-mounted submerged block. Their results showed that the sloshing in the system is highly sensitive to the frequency of tank motion. Some researchers also used a single vertical baffle. For example, Golla et al. (2021) experimentally studied the effect of three types of vertical baffles, including surface-piercing bottom-mounted, flush-mounted, and immersed bottom-mounted baffle configurations, on the sloshing noise in a rectangular tank in different sloshing regimes and various fill levels. Yu et al. (2020) conducted some experimental studies to find the optimum number and position of the vertical baffles to suppress the sloshing impact. Xue et al. (2017) experimentally investigated the effectiveness of different types of baffles in suppressing pressure under a wide range of frequencies. They measured the dynamic impact pressure alongside the central line of the tank wall for tanks without baffles and with different kinds of baffles, including perforated vertical baffles, surface-piercing bottom-mounted vertical baffles, vertical baffle flushing with a free surface, and immersed bottom-mounted vertical baffles. Some researchers also recently investigated the dual baffle. For instance, Cho and Kim (2016) also studied the effect of dual vertical baffles on sloshing reduction in a swaying rectangular tank. They showed that the submergence depth and baffle location are important parameters affecting the performance of the dual vertical baffles. Saghi et al. (2020b) evaluated the effectiveness of the oblique dual baffle on the sloshing impact arising from sway motion on the rectangular storage tank. They also examined the effect of baffle geometric parameters, including baffle position and orientation, and showed that the suggested optimum baffle can reduce sloshing loads by up to 15%. Ma et al. (2021) numerically studied suppressing the sloshing with single and dual vertical baffles. They showed that the spacing distance between the baffles is an important parameter; thus, the peak impact pressure from the sloshing phenomenon can be inhibited more than approximately three times low, thus producing dual baffles with a poor arrangement.

EG has been presented as an optimization tool by Bejan (1979; 1987) and was employed by other researchers in the last decade. For instance, Saghi and Lakzian (2017) and Saghi (2018) considered the EG criterion to optimize the 2D rectangular and elliptical storage tanks. They also applied EG in the dam-break flow with obstacles and found the optimum shape of the obstacle (Saghi and Lakzian 2019). EG was considered in this study as a criterion to compare different scenarios of the dual baffle. Therefore, the efficiency of the dual baffle is increased by decreasing EG. Therefore, the optimum dual baffle is related to the minimum EG. Along these lines, some parameters of dual baffles, including position and length, have been considered. Meanwhile, the researchers did not use the curved dual baffle.

A similar study was only conducted by Kamath et al. (2021) to evaluate the effects of the baffle on the sloshing. Different from their work for the effects of the single baffle on the sloshing in roll motion, the single- and dual-baffle effects on sloshing in sway motion were studied in the present paper, in which the baffle curvature and EG were considered. Therefore, a series of experimental and numerical tests are performed in this study to examine the effects of the curvature of the dual baffle in rectangular storage tanks on reducing the sloshing. The numerical model based on OpenFOAM is used to solve the unsteady incompressible RANS equations by using an interFoam solver and applied to the various dual-baffled configurations for the design optimization using some criteria including the total EG.

2 Experimental setup used to validate the numerical model

The experiments of a tank sloshing with single and dual baffles as the passive measures were conducted at Hakim Sabzevari University. Figure 1(a) shows the shake table used in the experiments, which is 1.35 m in length and 0.80 m in width. The thickness of the steel plate of the shake table body is 8 mm. An electric motor with 4 250.4 W power and 1450 r/min angular velocity is used in the power point system (Figure 1(b)). The shake table can generate a harmonic oscillation with a frequency below 10 Hz and 0–0.07 m amplitude. The liquid tank is 0.45 m in length, 0.15 m in width, and 0.30 m in height (Figure 1(c)). The storage tank comprises Plexiglas and is fixed on the shake

(a) Shake table (b) Driving motor (c) Storage tank

Figure 1 Experimental setup (Hakim Sabzevari University)

table. The thickness of the tank wall is 0.015 m; thus, the tank is rigid. The baffles comprise a glass with 0.003 m thickness. The width of the baffles is the same as the inner width of the tank (0.15 m). The height of the baffles is also variable (H_b = 0.02, 0.04, and 0.06 m). A digital camera is placed in front of the shake table to record the free surface oscillation. The "Aoao Video to Picture Converter" and "Plot digitizer" software are used to extract the required information from the photos taken.

3 Numerical Model description and boundary conditions

A 2D numerical study on the single and dual-baffled rectangular storage tanks was conducted in this paper to optimize against the sloshing phenomenon. The coordinate system of the tank without baffle and a pressure probe named *P*, which is in the middle of the tank, is shown in Figure 2(a). For comparison, the single baffle positioned at the tank center was also considered, as shown in Figure 2(b). The tank length is divided into two and three equal parts by the single and dual baffles, respectively. The variable H denotes the tank depth, H_w is the water depth, H_b is the baffle height, t_2 is the baffle thickness, and L is the length of the tank in the figure.

The fluid was considered viscous, incompressible, and laminar in the present study. Therefore, the Navier–Stokes equations can be used as the governing equations as follows (Versteeg and Malalasekera 2007):

$$\nabla \cdot \boldsymbol{U} = 0 \tag{1}$$

$$\frac{\partial \boldsymbol{U}}{\partial t} + \nabla \cdot (\boldsymbol{U}\boldsymbol{U}) - \nabla \cdot \left(\upsilon \cdot \left(\nabla \boldsymbol{U} + (\nabla \boldsymbol{U})^{\mathrm{T}} \right) \right) = \boldsymbol{g} - \frac{\nabla P}{\rho} \tag{2}$$

where U is the velocity vector, t is the time, v is the kinematic viscosity of the fluid, P is the dynamic pressure, and g is the gravitational acceleration.

The volume of fluid (VOF) method was used in this paper to describe scalar corresponding phase fields. The parameter α defined as Equation (3) is updated at each time step by using Equation (4). This equation was solved via the multidimensional universal limiter

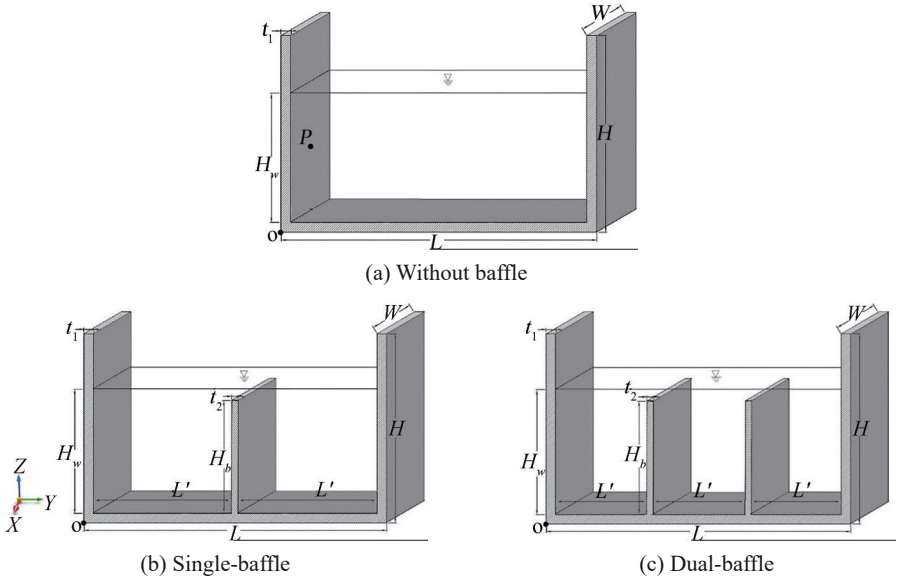

(a) Without baffle

(b) Single-baffle (c) Dual-baffle

Figure 2 Coordinate system of the baffled rectangular storage tank

for explicit solution method (Rudman 1997; Saghi and Ketabdari 2014; Ketabdari and Saghi 2013d; Ketabdari and Saghi 2012c):

$$\left\{\begin{array}{ll}\alpha = 0 & \text{air}\\ \alpha = 1 & \text{water}\\ 0 < \alpha < 1 & \text{interrface cell}\end{array}\right\} \tag{3}$$

$$\frac{\partial \alpha}{\partial t} + \nabla \cdot (\boldsymbol{U}\alpha) = 0 \tag{4}$$

where α is the quantity of water per unit of volume. OpenFOAM in version 7.0 is adopted in the present study to model the related sloshing phenomenon in the rectangular storage tank. First, the "interFoam" solver, which takes advantage of handling dynamic meshes for moving surfaces, is chosen to model the sway motion. In addition, "interFoam" can solve the three-dimensional Navier – Stokes equation for two incompressible phases using finite volume discretization and the VOF method. The solver algorithm called the pressure implicit method for the pressure-linked equation is a combination of pressure implicit with operator splitting and semi-implicit method for pressure-linked equation algorithms. Thus, "interFoam" is used in the present study due to its various advantages (OpenFOAM 2019). Time derivative terms were discretized by using the first-order implicit Euler discretization scheme. The second-order centered Gauss linear scheme was also used to discretize the gradient parameters. The skewness-corrected centered Gauss linear correction was employed for the Laplace derivative terms, and the upwind scheme was utilized to handle the divergence terms. The domain has been bounded by walls in this study. Hence, the velocity field, namely the movingWallVelocity boundary condition, was employed for these boundaries. By contrast, the fixedFluxPressure and zeroGradient boundary conditions were respectively implemented for the pressure field and the phase zone (OpenFOAM 2019).

The EG analysis is also adopted to investigate the irreversible aspects of the second law of thermodynamics and the effects of the new design on loss reduction. The fluid friction and heat transfer dissipation are both irreversible processes. The irreversibility for Newtonian fluids is introduced as local EG by Bejan (1979):

$$S'''_{\text{gen}} = \frac{k}{T_i^2}(\nabla T)^2 + \frac{\mu}{T_i}\varphi \tag{5}$$

where S'''_{gen} is the entropy generation rate, k is the fluid thermal conductivity, T_i is the fluid temperature, μ is the fluid dynamic viscosity, and φ is viscous dissipation function.

The temperature is considered ambient (i. e., 293 K) in this study. The temperature gradient is often negligible in rectangular storage tanks. Thus, the isothermal flow is focused on the sloshing phenomenon; only the EG created by the fluid friction is considered. The parameters of the viscous dissipation (φ) and the total EG (S_{gen}) are respectively defined as follows:

$$S_{\text{gen}} = \int_0^H \int_0^L \int_0^W \frac{\mu}{T_i}\varphi \mathrm{d}x\mathrm{d}y\mathrm{d}z = \sum_{i=1}^{N_x}\sum_{j=1}^{N_y}\sum_{k=1}^{N_z}\frac{\mu}{T_i}\varphi\Delta x\Delta y\Delta z \tag{6}$$

$$\varphi = 2\left[\left(\frac{\partial u}{\partial x}\right)^2 + \left(\frac{\partial v}{\partial y}\right)^2 + \left(\frac{\partial w}{\partial z}\right)^2\right] + \left(\frac{\partial u}{\partial y} + \frac{\partial v}{\partial x}\right)^2 + \left(\frac{\partial u}{\partial z} + \frac{\partial w}{\partial x}\right)^2 + \left(\frac{\partial v}{\partial z} + \frac{\partial w}{\partial y}\right)^2 \tag{7}$$

where u, v, and w are the velocity components, Δx, Δy, and Δz are the mesh size, and N_x, N_y, and N_z are the number of the meshes in the x-, y-, and z-directions, respectively.

The accumulated total EG ($S_{\text{gen,cum}}$) at time Tc is evaluated as:

$$S_{\text{gen,cum}} = \sum_{t=0}^{Tc} S_{\text{gen}} \tag{8}$$

4 Some tests to validate the numerical model

The dependence of the numerical results on the mesh size is first examined. Thus, a tank with H = 0.3 m, L = 0.45 m, W = 0.15 m, and H_w = 0.06 m (Figure 2(a)) undergoes harmonic sway motion with 0.04 m amplitude and 5 rad/s angular frequency. The horizontal force exerted on the tank was estimated at different mesh sizes, and the results are shown in Figure 3. These results indicate a mesh size independence for the mesh sizes smaller than 0.005 m. The sensitivity of time-step integration was estimated based on Courant number 0.5.

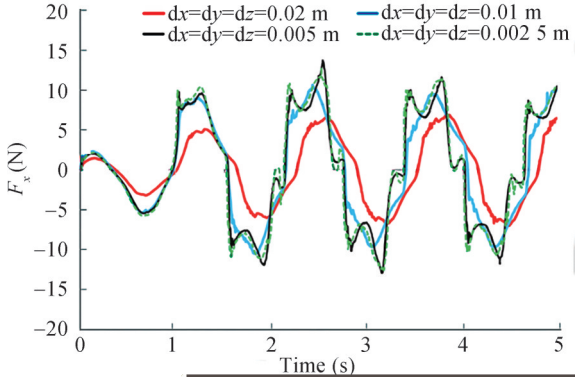

Figure 3 Horizontal force on the tank to evaluate the mesh size independence

In this step, different cases, including the simple tank (Figure 2(a)), single-baffled tank (Figure 2(b)), and dual-baffled tank (Figure 2(c)), were modeled under a harmonic sway motion, and the numerical model was validated by comparing with the experimental results obtained in the

present study. First, a sway motion with 0.04 m amplitude and 5 rad/s angular frequency was exerted on the simple tank, and the distribution of the surface elevation along the tank was then numerically and experimentally calculated as shown in Figures 4 and 5. The water depth in this test is 0.06 m. The results indicate a good consistency between the results.

As another test, a sway motion with 0.04 m amplitude and 5 rad/s angular frequency was exerted on the single-baffled tank, and the results are shown in Figures 6 and 7. In this test, H_b = 0.12 m, t_2 = 0.003 m, and H_w = 0.12 m. The results show that air is trapped in the rolled free surface at the tip of the baffle, which can be easily captured by the numerical model.

Finally, a harmonic sway motion of 0.04 m amplitude and 4.6 rad/s was exerted on the tank, and the distribution

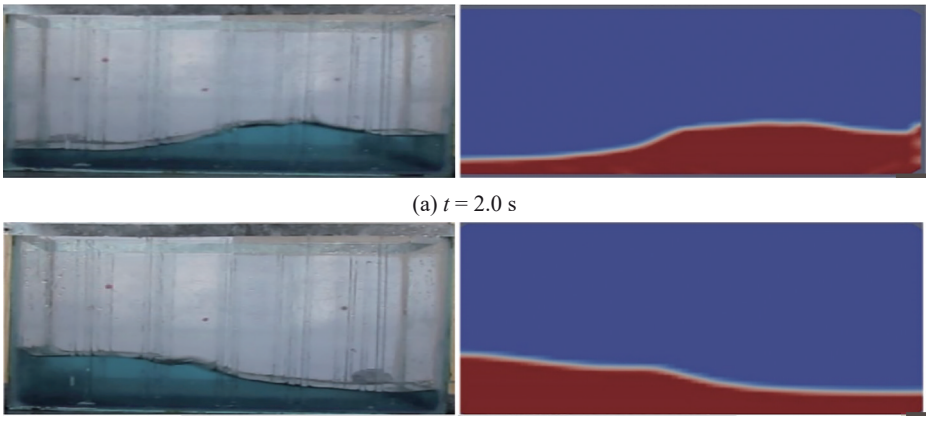

(a) t = 2.0 s

(b) t = 5.0 s

Figure 4 Snapshot of the free surface in a simple rectangular tank

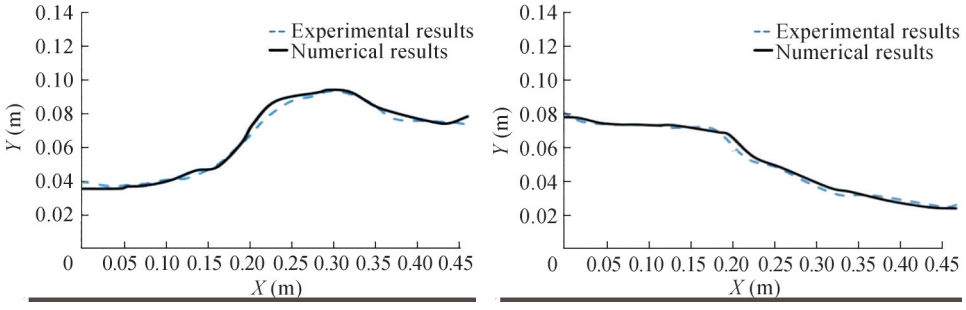

(a) t = 2.0 s (b) t = 5.0 s

Figure 5 Comparison of the free surface oscillation in a simple rectangular tank for the experimental and numerical results at t = 2.0 s and t = 5.0 s

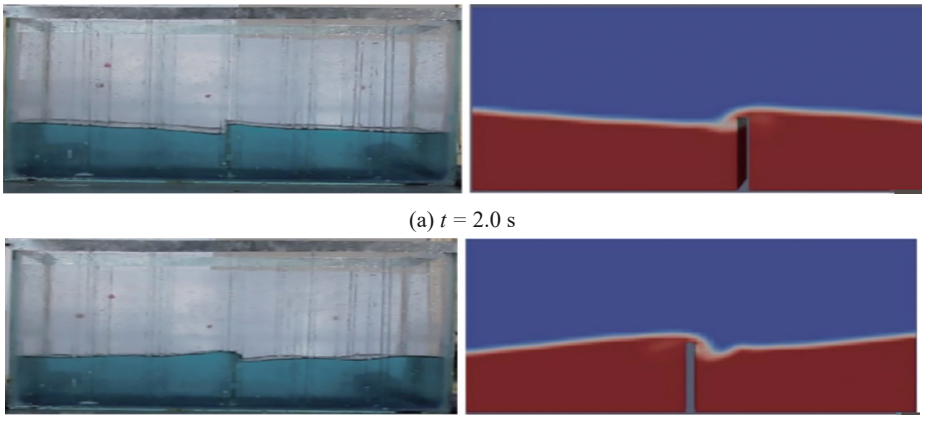

(a) t = 2.0 s

(b) t = 5.0 s

Figure 6 Snapshot of the free surface in a single-baffled rectangular tank

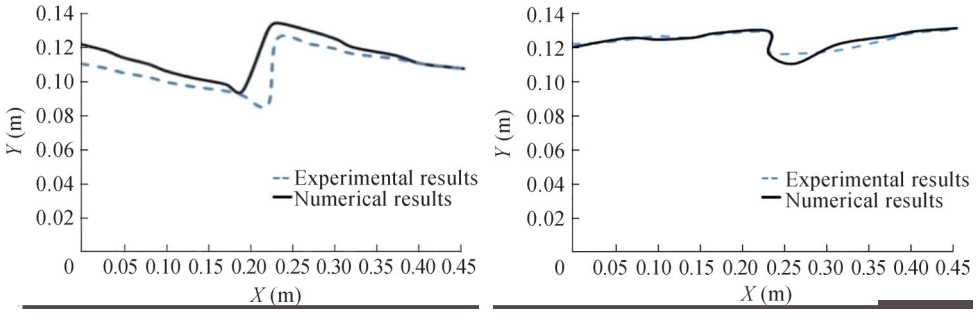

(a) $t = 2.0$ s (b) $t = 5.0$ s

Figure 7 Comparison of the free surface oscillation in a single-baffled rectangular tank for the experimental and numerical results at $t = 2.0$ s and $t = 5.0$ s

of the surface elevation along the tank from experimental and numerical results at $t = 2$ and 5 s are respectively shown in Figures. 8 and 9. In this test, $H_b = 0.12$ m, $t_2 = 0.003$ m, and $H_w = 0.12$m. The figures reveal the presence of similar phenomena between experimental and numerical simulations at different instants.

A sway motion of amplitude $a = 0.001$ m and $w = 5.83$ rad/s angular frequency was exerted on the tank with $H = 0.33$ m, $L = 0.48$ m length (Figure 2(a)), and $H_w = 0.09$ m to confirm that the model encapsulates effective sloshing pressure magnitudes applied on tank walls. The pressure at point P (Figure 2(a)) was calculated, and the results were compared with those of Xue et al. (2019) in Figure 10. A good agreement was found between the results.

5 Results and discussions

5.1 Effects of dual-baffle height

First, the effects of dual-baffle height were evaluated on the results of horizontal wave force on the tank. The tank parameters are the same as the tank with the single baffle (Figure 2(b)). A sway motion with 0.04 m amplitude and 5 rad/s angular frequency was exerted on the tank. The static water depth was selected as 0.06 m. The dual-baffle height and thickness were considered as $H_b = 0.01$, 0.03, and 0.06 m and $t_2 = 0.003$ m, respectively. The single baffle with the same heights positioned at the tank center, named as a middle baffle, was also modeled separately to compare their effects on reducing the sloshing phenomenon. The related results are shown in Figure 11. This figure reveals that the difference among results with and without baffles is quite small for the baffle height $H_b = 0.01$ m, as shown in Figure 11(a). Thus, the baffle effect of sloshing reduction can be neglected for small baffle heights. The results of horizontal wave forces on the tank become smaller than that without baffle and tend to stabilize with the further increase in baffle height, especially for the dual-baffle case, as shown in Figure 11(c).

The maximum horizontal force exerted on the tank ($F_{x\max}$) and the decrement percentage of maximum horizontal force (DF) were calculated for different baffle heights based on the obtained results, and the findings are shown in Figure 12. The parameter DF is calculated as follows:

$$\mathrm{DF} = \frac{F_{x\max} - F_{x\max b}}{F_{x\max}} \tag{9}$$

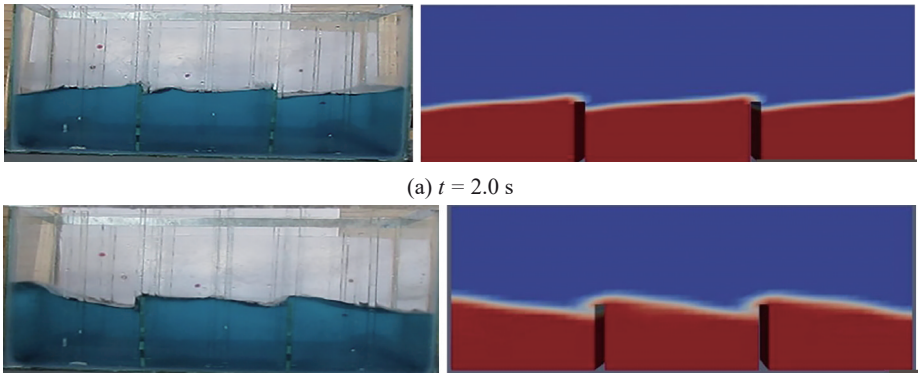

(a) $t = 2.0$ s (b) $t = 5.0$ s

Figure 8 Comparison of the free surface in the rectangular tank between experimental results and numerical results at different time instants

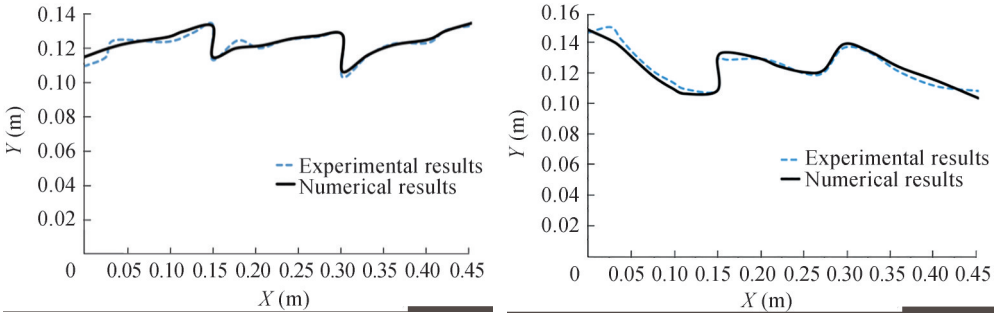

(a) t = 2.0 s (b) t = 5.0 s

Figure 9 Comparison of the free surface oscillation for experimental and numerical results

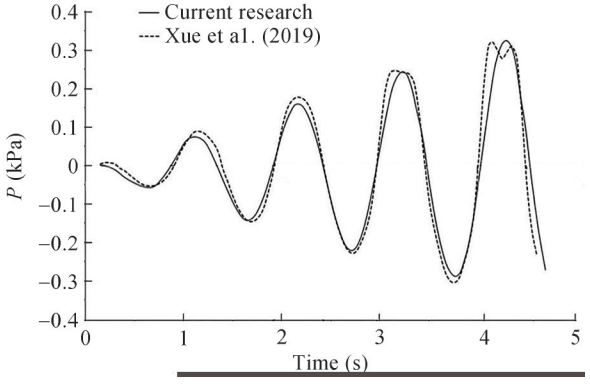

Figure 10 Comparison of the pressure data between the results of the current paper and those of Xue et al. (2019)

where F_{xmaxb} is the maximum horizontal force exerted on the simple tank (without baffle). The F_{xmax} is calculated based on the horizontal force exerted on the tank perimeter during the simulation. The horizontal force exerted on the tank is estimated as follows:

$$F_x = \int_A p n_x \mathrm{d}A \tag{10}$$

where n_x is the component of the unit vector perpendicular to the tank surface in the x-direction, p is the dynamic pressure on the tank perimeter, and A is the element area on the wet tank surface.

The results in Figure 12(b) indicate that the parameter DF of the dual-baffled tank (Figure 2(c)) for $H_b/H_w > 0.5$ is more than that of the single-baffled tank (Figure 2(b)). Therefore, the baffle effect on reducing the sloshing is observed for the dual baffle compared with the single baffle

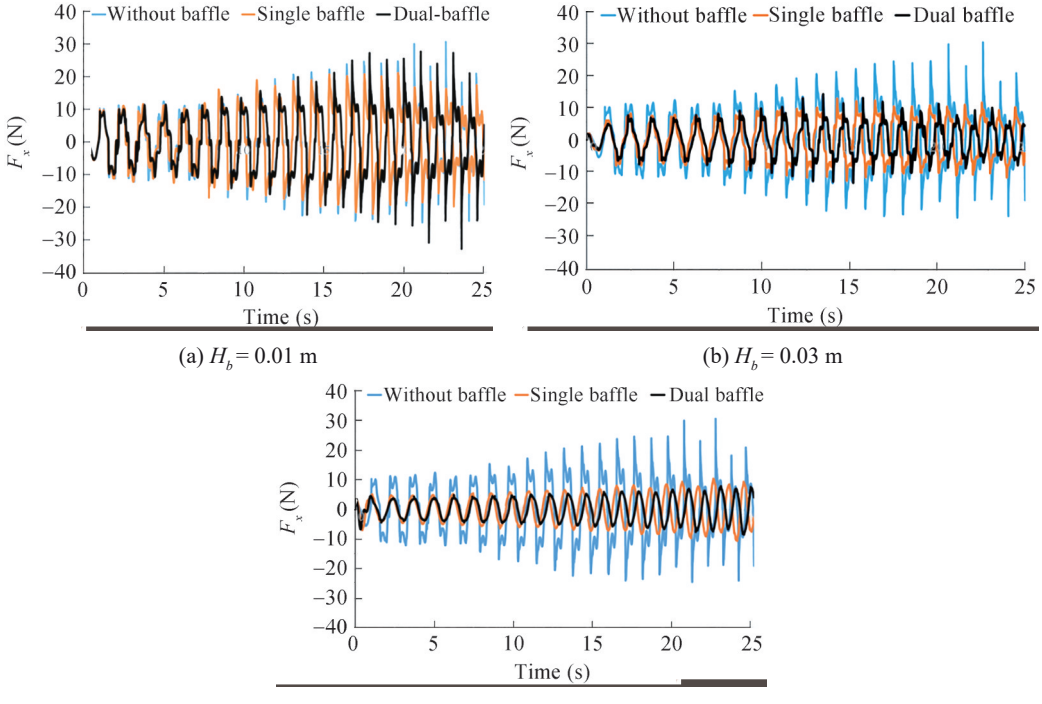

(a) H_b = 0.01 m (b) H_b = 0.03 m

(c) H_b = 0.06 m

Figure 11 Effect of baffle height on the horizontal force exerted on the tank

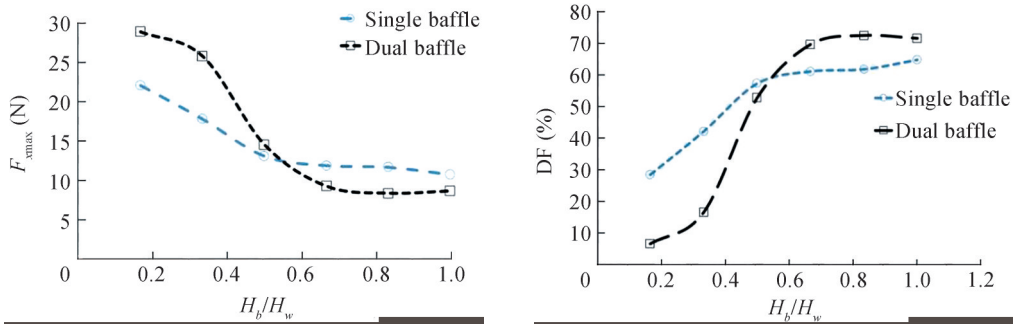

(a) Maximum horizontal force (b) Decrement percentage of maximum horizontal force

Figure 12 The effects of the baffle height on the maximum horizontal force exerted on the tank

positioned at the tank center. However, the effects of a single baffle are more substantial than those of a dual baffle when the relative baffle height $H_b/H_w < 0.5$. Finally, the results show that the effects of single and dual baffles are nearly constant when the relative baffle height $H_b/H_w > 0.75$.

The EG was estimated for the storage tanks with different dual-baffle heights based on Eq. (9), and some results are shown in Figure 13(a). The variation of the total cumulative EG with baffle height is also shown in Figure 13(b). The baffle effect is also constant as the relative baffle height $H_b/H_w > 0.75$, which is in accordance with Figure 12. Therefore, an adaptable baffle length can be selected based on practical engineering.

5.2 Effects of sway motion parameters

The effects of sway motion amplitude on the sloshing reduction with single and dual baffles were evaluated in this subsection. The different motion amplitudes (a = 0.01, 0.02, 0.03, and 0.04 m) and 1.36 rad/s were exerted on the rectangular storage tank with the static water depth of 0.06 m. The baffle height and thickness were H_b = 0.06 m and t_2 = 0.003 m, respectively. The horizontal force exerted on the tank was then estimated for different sway motion amplitudes. The parameter DF was calculated for different sway motion amplitudes (a) based on the obtained results, and the findings are shown in Figure 14(a). DF decreases with the motion amplitude when $a < 0.03$ m, which means that the effect of sloshing reduction is apparent. However, the variation trend is the opposite; that is, DF starts to increase slowly when $a > 0.03$ m. Furthermore, EG was estimated for the dual baffle and different sway motion amplitudes, as shown in Figure 14(b). The results show that the EG increases with the increment of sway motion amplitude.

The effects of sway motion frequency on DF were evaluated. The sway motion with 0.04 m amplitude and different frequencies were exerted on the rectangular storage tank with a static water depth of 0.06 m. The horizontal force exerted on the tank was estimated for different sway motion frequencies. The decrement percentage of maximum horizontal force (DF) was calculated for different sway motion frequencies (f) based on the obtained results, and the findings are shown in Figure 14(c). The results also reveal that the effect of dual baffle relative to middle single baffle is observed in the low angular frequencies and is only slightly evident in the high angular frequencies.

6 Optimization of inclined and curved dual-baffle configurations

This section aims to examine the effects of different designs of the dual-baffled water tanks on sloshing. Three designs include one inclined straight and two curved baffle designs, as shown in Figure 15. The dual straight and

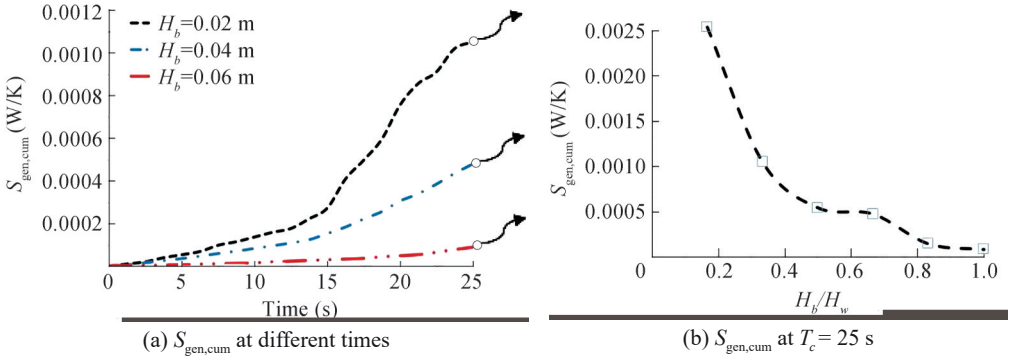

(a) $S_{gen,cum}$ at different times (b) $S_{gen,cum}$ at T_c = 25 s

Figure 13 $S_{gen,cum}$ for the storage tanks with different dual baffle heights

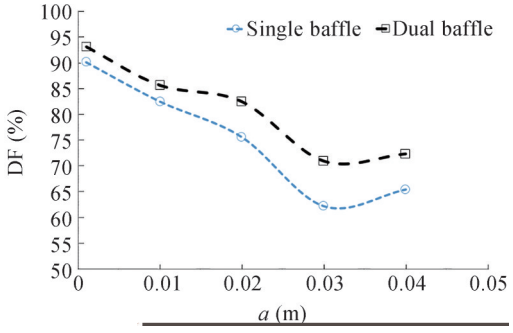

(a) Distribution of the decrement percentage of maximum horizontal force (DF) with sway motion amplitude

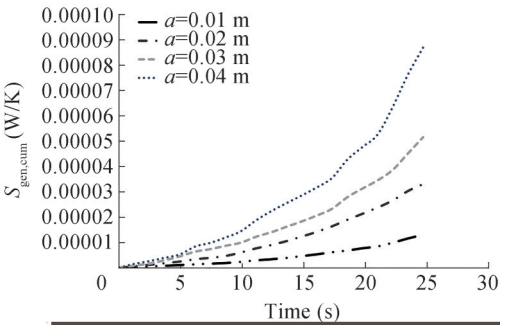

(b) Accumulative EG for different sway motion amplitudes (a)

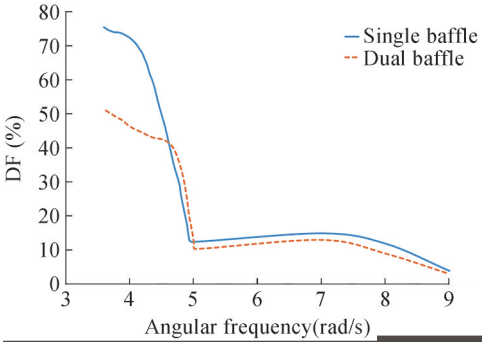

(c) Decrement percentage of maximum horizontal force (DF)

Figure 14 The effects of sway motion frequency on DF

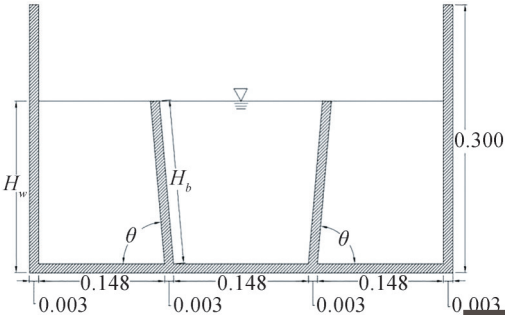

(a) Inclined dual-baffle

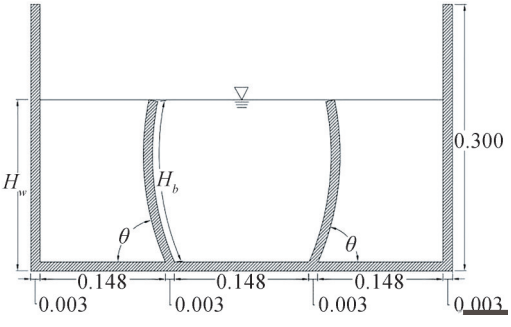

(b) Inner curved dual-baffle

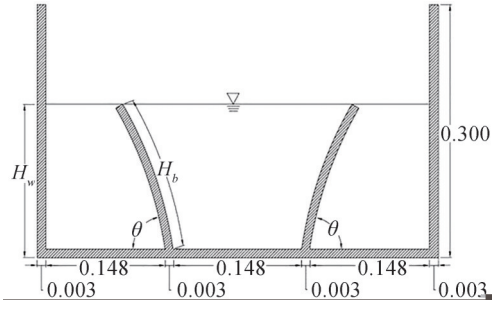

(c) Outer curved dual-baffle

Figure 15 Sketch of the dual baffle

curved baffles (i. e., inner and outer curved baffles) inclined with different inclination angles are designed with the following equations:

$$y = 673x^2 - 401.95x + 60 \quad (11)$$

$$y = -839x^2 + 2105x - 13 \quad (12)$$

In these experiments, the sway motion with 0.04 m amplitude and 1.36 Hz frequency is applied on a rectangular storage tank with the initial water depths of 0.06 m and 0.18 m. The dual-baffle height (H_b) varies between 0.01 and 0.06 m, and the thickness (t_2) is maintained at 0.003 m.

The maximum horizontal force and EG were estimated for different inclination angles (θ = 65°, 75°, 85°, 95°, 105°) for the inclined straight dual-baffle configuration shown in Figure 15(a), and the results are shown in Figure 16. The value of EG and maximum horizontal force in the rectangular storage tank with 80° and 85° inclination angles is the smallest compared with the other inclination angles for H_w = 0.06 m and 0.18 m, respectively.

The two configurations in Figures 15(b) and 15(c) are used in the rectangular storage tanks (case 1) to evaluate the efforts of the curved baffle configurations on the sloshing reduction. The water depth is set to 0.18 m. The sway motion used in this set of tests is similar to that previously used (0.04 m amplitude and 1.36 rad/s frequency). The results of horizontal force exerted on the tank and EG are estimated and compared with the inclined dual baffle, as shown in Figure 17. The results in Figure 17(a) indicate that the maximum horizontal force exerted on the tank for inclined dual baffle is 24.66 N, while those for the curved dual baffles shown in Figures 15(b) and 15(c) are 22.13 and 20.61 N, respectively. Thus, using the curved dual baffle can further decrease the maximum horizontal force exerted on the tank by around 10%–16% in this study. Figure 17(b) shows that using the curved dual baffle can increase *EG* by around 10% and decrease EG by around 20% for the two cases. Therefore, the curved dual baffle shown in Figure 15 (c) is suggested as the optimum dual baffle.

The distributions of EG in the tanks with inclined and curved dual baffles at an inclination angle of 85° (Figure 15) are shown in Figure 18 at the selected time steps. The results show that the distribution of EG in the rectangular storage tank with curved dual baffles is less than that with inclined dual baffles.

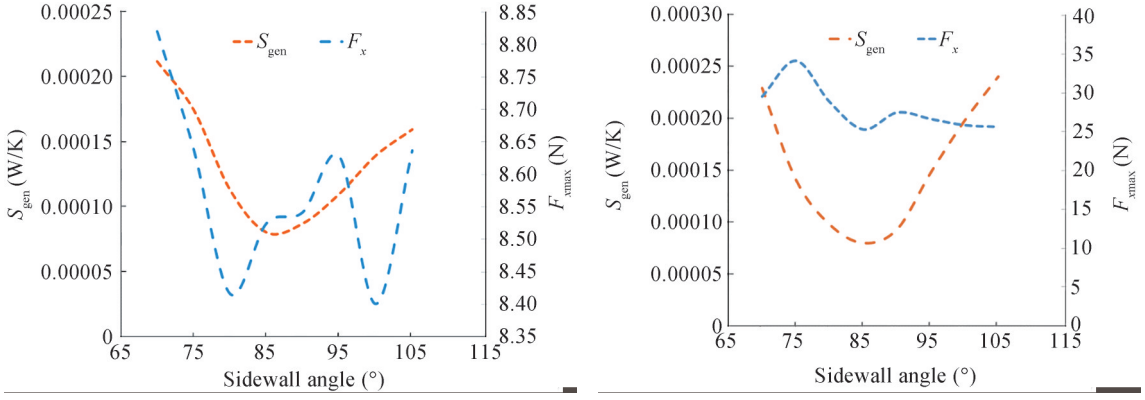

(a) H_w = 0.06 m (b) H_w = 0.18 m

Figure 16 Variation of the maximum horizontal force and EG with inclination angle at H_w = 0.06 m and H_w = 0.18 m

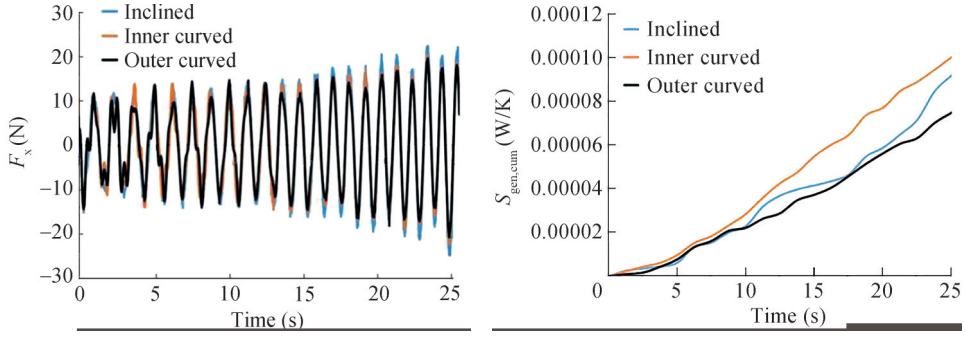

(a) Horizontal force exerted on the tank (b) $S_{gen,cum}$ different times

Figure 17 Comparison of inclined and curved dual baffles with a sidewall angle of 85°

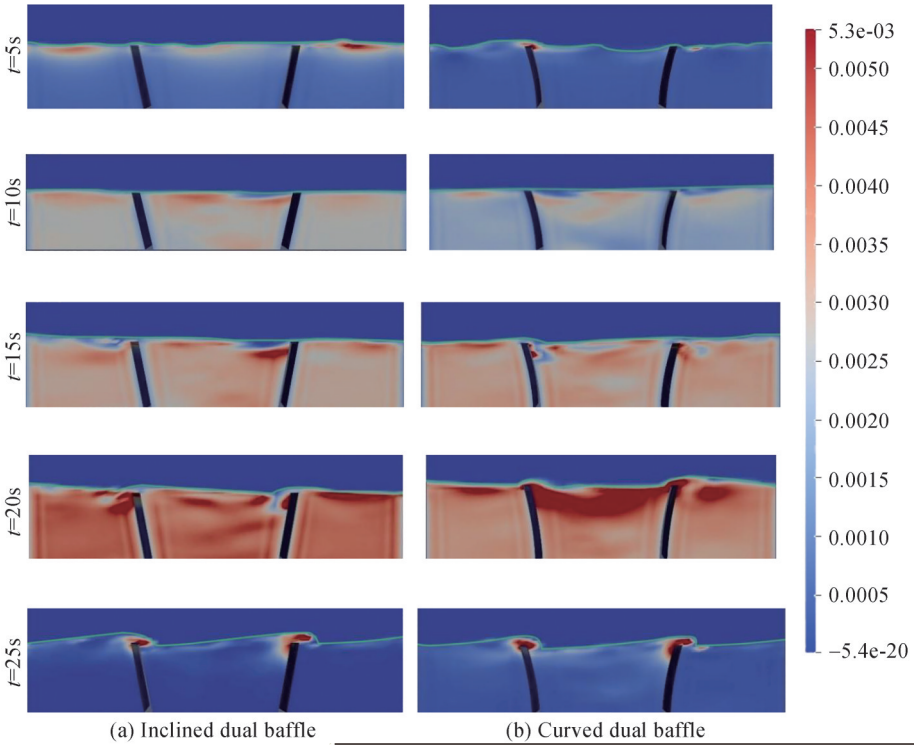

Figure 18 Snapshots of the *EG* distribution at different times and for the optimum rectangular storage tanks

7 Conclusions

A series of numerical and experimental tests were performed in this study to model the sloshing phenomenon in the dual-baffled rectangular storage tanks. The dual-baffled rectangular storage tank was optimized based on some criteria, which comprise the maximum horizontal force exerted on the tank and EG. The results show that the dual-baffled tank is more effective than the single-baffled one in sloshing reduction when the relative baffle height $H_b/H_w >$ 0.5, while such an effect is constant when the relative baffle height $H_b/H_w > 0.75$, where dual- and single-baffled configurations have nearly the same effect in sloshing reduction. The results also show that the EG decreases with the increment of the baffle height. Furthermore, the decrement percentage of the maximum horizontal force (DF) is the same for single and dual-baffled tanks when the sway motion amplitude is $a < 0.03$ m, where the parameter DF reaches the minimum, during the evaluation of the effects of sway motion amplitude and frequency on the sloshing. The dual-baffle effect on reducing the sloshing is more substantial compared with the single-baffle in the low angular frequencies and is only minimal in the high angular frequencies considering the angular frequency of the sway motion.

The inclined and curved dual baffled rectangular tanks with different sidewall angles were also considered in this study for optimization. The results show that the horizontal force is minimum for the sidewall angle of 80° at the cases of shallow water depth. However, the horizontal force was found to be minimum at the sidewall angle of 85° with the increase in the water depth. The EG is always minimum at the sidewall angle of 85°. Therefore, the sidewall angle of 85° is selected as the optimum sidewall angle. Finally, the curved dual baffle with different curve equations was investigated. The results show that the optimum curved dual baffle decreases the horizontal force exerted on the tank by around 10% – 15% considering inclined dual baffle. Furthermore, using this curved dual baffle decreases EG by around 20%. Therefore, the curved dual baffle is suggested as the optimum dual baffle.

References

Abramson HN (1996) The dynamic behavior of liquids in moving containers. NASA, SP-106 National Aeronautics and Space Administration, Washington D.C.

Bejan A (1979) A Study of entropy generation in fundamental convective heat transfer. J Heat Transf. 101(4): 718-725. DOI: 10.1115/1.3451063

Bejan A (1987) The thermodynamic design of heat and mass transfer processes and devices. Int J Heat Fluid Flow 8: 258-276

Chen BF, Nokes R (2005) Time-independent finite difference analysis of fully nonlinear and viscous fluid sloshing in a rectangular tank. J Comput Phys. 209(1): 47-81. DOI: 10.1016/j.jcp.2005.03.006

Cho IH, Kim MH (2016) Effect of dual vertical porous baffles on sloshing reduction in a swaying rectangular tank. Ocean Engineering 126: 364-373. DOI: 10.1016/j.oceaneng.2016.09.004

Curadelli O, Ambrosini D, Mirasso A, Amani M (2010) Resonant

frequencies in an elevated spherical container partially filled with water: FEM and measurement. J. Fluids Struct. 26(1): 148-159. DOI: 10.1016/j.jfluidstructs.2009.10.002

Frandsen JB (2004) Sloshing motions in excited tank. J Comput. Phys. 196(1): 53-87. DOI: 10.1016/j.jcp.2003.10.031

Gavrilyuk IP, Lukovsky IA, Timokha AN (2005) Linear and nonlinear sloshing in a circular conical tank. Fluid Dyn. Res. 37(6): 399-429. DOI: 10.1016/j.fluiddyn.2005.08.004

Golla ST, Ventakesham B (2021) Experimental study on the effect of centrally positioned vertical baffles on sloshing noise in a rectangular tank. Applied Acoustic 176: 107890. DOI: 10.1016/j.apacoust.2020.107890

Hasheminejad SM, Aghabeigi M (2012) Sloshing characteristics in half-full horizontal elliptical tanks with vertical baffles. Appl Math Model 36(1): 57-71. DOI: 10.1016/j.apm.2011.02.026

Jung JH, Yoon HS, Lee SY, Shin SC (2012) Effect of the vertical baf fl e height on the liquid sloshing in a three-dimensional rectangular tank. Ocean Engineering 44: 79-89. DOI: 10.1016/j.oceaneng.2012.01.034

Kamath A, Liavåg Grotle E, Bihs H (2021) Numerical investigation of sloshing under roll excitation at shallow liquid depths and the effect of baffles. Journal of Marine Science and Application 20: 185-200. DOI: 10.1007/s11804-021-00198-y

Ketabdari MJ, Saghi H (2012a) Numerical analysis of trapezoidal storage tank due to liquid sloshing phenomenon. Iran J Mar Sci Technol. 18: 33-39

Ketabdari MJ, Saghi H (2012b) A novel algorithm of advection procedure in volume of fluid method to model free surface flows. International Scholarly Research Network ISRN Applied Mathematics 12: ID 521012. DOI: 10.5402/2012/521012

Ketabdari MJ, Saghi H (2013a) Parametric study for optimization of storage tanks considering sloshing phenomenon using coupled BEM–FEM. Appl. Math. Comput. 224: 123-139. DOI: 10.1016/j.amc.2013.08.036

Ketabdari MJ, Saghi H (2013b) Numerical study on behavior of the trapezoidal storage tank due to liquid sloshing impact. Int J. Comput. Methods 10(6): 1-22. DOI: 10.1142/S0219876213500461

Ketabdari MJ, Saghi H (2013c) A new arrangement with nonlinear sidewalls for tanker ship storage panels. J Ocean Univ. China 12(1): 23-31. DOI: 10.1007/s11802-013-1925-2

Ketabdari MJ, Saghi H (2013d) Development of volume of fluid methods to model free surface flow using new advection algorithm. J Braz. Soc. Mech. Sci. Eng. 35(4): 479-491. DOI:10.1007/s40430-013-0045-7

Ketabdari MJ, Saghi H, Rezaei H, Rezanejad K (2015) Optimization of linear and nonlinear sidewall storage Units Coupled boundary element-finite element methods. KSCE J Civ Eng. 19(4): 805-813. DOI: 10.1007/s12205-011-0396-5

Ma C, Xiong C, Ma G (2021) Numerical study on suppressing violent transient sloshing with single and double vertical baffles. Ocean Engineering 223: 108557. DOI: 10.1016/j.oceaneng.2020.108557

Nayak SK, Biswal KC (2015) Fluid damping in rectangular tank fitted with various internal objects–An experimental investigation. Ocean Engineering 108: 552-562. DOI: 10.1016/j.oceaneng.2015.08.042

Ning DZ, Song WH, Liu YL, Teng B (2012) A boundary element investigation of liquid sloshing in coupled horizontal and vertical excitation. Journal of Applied Mathematics vol. 2012, Article ID 340640. DOI: 10.1155/2012/340640

OpenFOAM (2019) The openFoam Foundation, User Guide, http://openfoam.org

Papaspyrou S, Karamanos SA, Valougeorgis D (2004) Response of half-full horizontal cylinders under transverse excitation. J Fluids Struct. 19: 985-1003. DOI: 10.1016/j.jfluidstructs.2004.04.014

Rudman M (1997) Volume-tracking methods for interfacial flow calculations. International Journal for Numerical Methods in Fluids 24: 671-691. DOI: 10.1002/(SICI)1097-0363(19970415)24: 7

Saghi H, Ketabdari MJ (2012) Numerical simulation of sloshing in rectangular storage tank using coupled FEM-BEM. J Mar Sci Appl. 11(4): 417-426. DOI: 10.1007/s11804-012-1151-0

Saghi H, Ketabdari MJ (2014) A modification to SLIC and PLIC volume of fluid models using new advection method. Arabian Journal for Science and Engineering 39: 669-684. DOI: 10.1007/S13369-013-0688-9

Saghi H (2016) The pressure distribution on the rectangular and trapezoidal storage tanks' perimeters due to liquid sloshing phenomenon. Int J Nav Archit. Ocean Eng. 8(2): 153-168. DOI: 10.1016/j.ijnaoe.2015.12.001

Saghi H, Lakzian E (2017) Optimization of the rectangular storage tanks for the sloshing phenomena based on the entropy generation minimization. Energy 128: 564-574. DOI: 10.1016/j.energy.2017.04.075

Saghi H (2018) Entropy generation minimization for the sloshing phenomenon in half-full elliptical storage tanks. Physica A: Statistical Mechanics and its Applications 491: 972-983. DOI: 10.1016/j.physa.2017.09.086

Saghi H, Lakzian E (2019) Effects of sing obstacles on the dam-break flow based on entropy generation analysis. European Physical Journal Plus 134(5): 124-137. DOI: 10.1140/epjp/i2019-12592-3

Saghi H, Ning DZ, Cong PW, Zhao M (2020a) Optimization of baffled rectangular and prismatic storage tank against the sloshing phenomenon. China Ocean Engineering 34(5): 1-13. DOI: 10.1007/s13344-020-0059-8

Saghi H, Mikolla T, Hirdaris S (2020b) The influence of obliquely perforated dual-baffles on sway induced tank sloshing dynamics. Proceedings of the Institution of Mechanical Engineers, Part M: Journal of Engineering for the Maritime Environment 235(4): 905-920. DOI: 10.1177/1475090220961920

Saghi R, Hirdaris S, Saghi H (2021) The influence of flexible fluid structure interactions on sway induced tank sloshing dynamics. Engineering Analysis with Boundary Elements 131: 206-217. DOI: 10.1016/j.enganabound.2021.06.023

Shekari MR, Khaji N, Ahmadi MT (2009) A couple BE-FE study for evaluation of seismically isolated cylindrical liquid storage tanks considering fluid-structure interaction. J Fluids Struct. 25(3): 567-585. DOI: 10.1016/j.jfluidstructs.2008.07.005

Versteeg HK, Malalasekera W (2007) An introduction to computational fluid dynamics the finite volume method. Pearson Education Limited, Edinburgh Gate, Harlow. Pages 495

Wu CH, Faltinsen OM, Chen BF (2012) Numerical study of sloshing liquid in tanks with baffles by time-independent finite difference and fictitious cell method. Comput. Fluids 63: 9-26. DOI: 10.1016/j.compfluid.2012.02.018

Xue MA, Zheng J, Lin P, Yuan X (2017) Experimental study on vertical baffles of different configurations in suppressing sloshing pressure. Ocean Engineering 136: 178-189. DOI: 10.1016/j.oceaneng.2017.03.031

Xue MA, Chen Y, Zheng J Qian L, Yuan X (2019) Fluid dynamics analysis of sloshing pressure distribution in storage vessels of different shapes. Ocean Engineering 192: 106582

Yue BZ (2008) Nonlinear coupling dynamics of liquid filled spherical container in microgravity. Appl. Math. Mech. 29(8): 983-990

Yu L, Xue, MA, Jiang Z (2020) Experimental investigation of parametric sloshing in a tank with vertical baffles. Ocean Engineering, 213: 107783. DOI: 10.1016/j.oceaneng.2020.107783